An Elastoplastic Analysis of Anchored Walls

Analyse Elastoplastique des Parois d'Ancrage

U. ARSLAN
H. BRETH
R. WANNINGER

Technical University of Darmstadt, Federal Republic of Germany

SYNOPSIS Material models used today for finite element analyses in engineering practice are still unsatisfactory. The interaction of the soil-wall-anchor system includes the behaviour of the ground level and of existing structures which are influenced by an excavation. Reliable conclusions from finite element analyses can be drawn only if the constitutive law of the soil incorporates the main characteristics of soil behaviour. The aim of this paper is to demonstrate that advanced constitutive laws are necessary and useful for simulation of anchored wall behaviour. A model is presented which is well suited for interaction analysis. Earth pressure distribution and deformations are discussed.

INTRODUCTION

Tie-back anchors for vertical cut slopes in soft ground have been in use for about two decades. They have been accepted as a useful technique in foundation engineering. The use of tie-backs for construction of deep excavations is a standard method which continuously substitutes the use of struts for supporting earth pressure loads. Strutted excavations can still be found in small excavations and at difficult subsoil conditions. In the course of time engineers have learned which soil conditions and which situations are difficult for anchored walls. Much experience has been gained in recent years. In the beginning and with the first applications of wall anchoring technique engineers had very little experience about the size and distribution of earth pressure. The mode of interaction between wall deformation and earth pressure distribution was only basically known. Since then a large number of measurements has been published. They provide deformation and earth pressure data of anchored walls and permit us to judge the basic differences between anchored and strutted excavations. These measurements in situ have, however, one decisive disadvantage: they are only valid for soil conditions and construction procedures at the place of measurement. An application of experience to other types of soil is difficult. Measurements in situ are expensive and very often inconvenient for construction work. To avoid these difficulties large series of model tests have been carried out in the past; e.g. Wanoschek and Breth (1972) and Breth and Wolff (1976). Numerical methods such as the finite element method make possible systematic investigations at exactly defined boundary conditions and require less costs than model tests. However, model tests are carried out with actual material, such as sand e.g., while "numerical models" incorporate soil via a constitutive law with experimentally determined parameters. The results of finite element analyses are decisively influenced by material law. The problem of appropriate constitutive laws is the central aspect of numerical analysis. Before interpreting any results of numerical analyses, the constitutive model should be carefully examined.

AN ELASTOPLASTIC CONSTITUTIVE MODEL

The stress-strain behaviour of cohesionless soil in general is nonlinear, inelastic, and dependent on stress path and previous stress history. Soil deformations during primary loading are largely irrecoverable. The sum of irrecoverable strains on a stress path defines the mechanical state of soil at the end of this stress path. Due to the inherently inelastic behaviour of soil, which results mainly from slidings between soil particles, the influence of stress history on the stress-strain behaviour is quite significant. The strains induced by given changes in stress can vary considerably depending on stress level, confining stress and depending on whether the stress changes involve primary loading, unloading or reloading (Breth, Chambosse and Arslan 1978). In addition, frictional materials such as soils, exhibit in dense state an expansion in volume under shearing (dilatancy). The essential aspects of stress-strain-strength behaviour of cohesionless soils under effective stresses can be summarized as follows:

- nonlinearity of stress-strain relations;
- gradual decrease in stiffness with increasing stress levels;
- irreversibility of portion of strains (this type of behaviour is characteristic for plastic materials);
- influence of minor principal stress ( ) on stress-strain behaviour;
- influence of intermediate principal stress (σ_2) on stress-strain behaviour and strength (Lade and Duncan 1973);
- shear-dilatancy effects;
- stress path dependency;
- coincidence of strain increment and stress increment axes at low stress levels with transition to coincidence of strain increments and stress axes at high stress levels by reorientation of stress axes due to shearing (Roscoe 1970).

The shortcomings of the Mohr-Coulomb failure criterion for soils have become evident since results from threedimensional tests became available. New failure criteria have therefore been suggested for soils (Lomize and Kryzhanovsky 1967; Matsuoka and Nakai 1977; Lade and Duncan 1975; Gudehus 1973).

Based on the results of cubical triaxial tests Lade and Duncan (1973) suggested a failure criterion for cohesionless soils in terms of the first and the third stress invariant:

$$I_1^3 - k_1 \cdot I_3 = 0$$

which also may be expressed as a stress level f_1:

$$f_1 = \frac{I_1^3}{I_3}$$

The value of f_1 varies from $f_{1T} = 27$ for hydrostatic stress conditions up to a value of k_1 at failure. In principal stress space the failure criterion is represented by a cone with the apex at the origin of the stress axes as shown in Fig. 1. This failure criterion models quite well the effective strength of dense sand which is inherently isotropic. For loose sand the condition of isotropy is not satisfied because sand in a loose state has an anisotropic fabric. This results in anisotropic mechanical behaviour under loading.

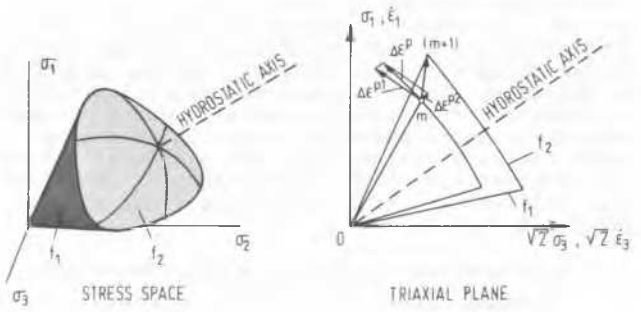

Fig. 1 Doublehardening Model

A realistic constitutive model of soil stress-strain-strength behaviour must account for the experimental observations mentioned above. They can be characterized by elements of the theory of plasticity which provides a convenient framework for the modelling of soil behaviour. In the incremental plasticity theory used in the elasto-plastic analyses of soil masses, it is generally assumed that the total strain increment is divided into an elastic and a plastic component

$$\{\Delta\varepsilon\} = \{\Delta\varepsilon^e\} + \{\Delta\varepsilon^p\}$$

The elastic strain is calculated separately by the generalized Hooke's law:

$$\{\Delta\varepsilon^e\} = [D^e]^{-1} \{\Delta\sigma\}$$

where $[D^e]$ is the elastic matrix. The development of the plastic stress-strain relations for soils is based on the concept of plasticity theory, e.g. as outlined by Hill (1950).

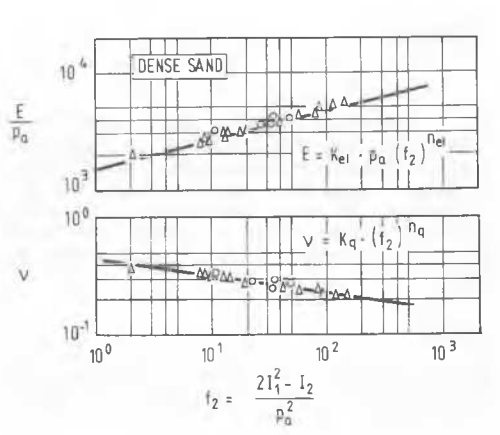

Fig. 2 Variation of Elastic Parameters with Stress State

Elastic Strains

The elastic parameters for calculation of elastic strains have often been gained from unloading and reloading in the conventional triaxial compression test. It should be mentioned, however, that sand, during unloading and reloading, follows a hysteresis loop. This loop does not exist if only small stress reversals are performed. In the model presented here, elastic parameters gained from small stress reversals in the triaxial compression test are described by an empirical law (Fig. 2). The elastic parameters E (elastic modulus) and ν (Poisson's ratio) are related to a scalar function of stress state as

$$\frac{2I_1^2 - I_2}{p_a^2}$$

where I_1 and I_2 are the first and second stress invariant and p_a is atmospheric pressure expressed in the same units as stresses and elastic modulus.

Plastic Strains

Within the theory of isotropic hardening (Hill 1950) plastic strains are defined by means of a yield surface, a flow rule and a workhardening law. The yield surface may change in size, position or shape as the soil is loaded successively to higher stress levels. The magnitude of this change depends on plastic work used to produce plastic yield. The relationship between plastic work and stress level is called workhardening law. The flow rule describes plastic strain increments apart from a multiplier. It is derived

from the requirement that the plastic strain increment direction should be normal to the plastic potential surface. The flow rule is said to be associated when the plastic potential surface coincides with the yield surface. Along the lines of plasticity theory together with isotropic hardening, different models have been developed for the formulation of elastoplastic stress-strain relations for sand; e.g. by Lade and Duncan (1975). Recently the idea of describing the plastic strains as the sum of two independent parts was introduced into soil mechanics to reflect better the experimental findings. The doublehardening constitutive model used in the elastoplastic analysis herein has two yield surfaces. The plastic strain is considered to consist of two components: contractive-plastic and dilative-plastic strains. The yield surfaces for the two plastic strain components are indicated in stress space and on a section through the stress space (triaxial plane) in Fig. 1. The cone with its apex at the origin of the stress space (after Lade) describes dilative-plastic strain components. The ellipsoid with centre also at space origin describes contractive-plastic strain components. As plastic yielding occurs during a loading process, the yield surfaces expand successively in the stress space, and the corresponding yield functions change their values.

An expansion of the elliptical yield cap is described by means of an associated flow rule:

$$\Delta\varepsilon_{ij}^{p2} = \Delta\lambda_2 \frac{\partial f_2}{\partial\sigma_{ij}} \cdot p_a^2 \qquad (*)$$

and by a hyperbolic relationship as an empirical workhardening law. It can be determined from an isotropic compression test as shown in Fig. 3.

$$\frac{W_{p2}}{p_a} = \frac{f_2}{M + L \cdot f_2}$$

M and L are dimensionless constants of the workhardening law. The value of the proportionality factor $\Delta\lambda_2$ in Eq.(*) can be written as

$$\Delta\lambda_2 = \frac{\Delta W_{p2}}{2 \cdot f_2 \cdot p_a^2}$$

A positive change of the function for the conical yield surface during a loading process performs the dilative component of plastic strain, which is described by a nonassociated flow rule:

$$\Delta\varepsilon_{ij}^{p1} = \Delta\lambda_1 \frac{\partial g_1}{\partial\sigma_{ij}}$$

g_1 is the plastic potential function of a form similar to the yield criterion:

$$g_1 = I_1^3 - k_2 \cdot I_3$$

where k_2 is constant for given values of f_1. The values of dilative-plastic work W_{p1} are determined from the results of conventional triaxial compression tests. Its variation with f_1 can be approximated by the function

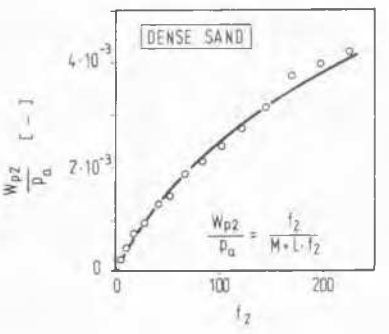

Fig. 3 Variation of Contractive-Plastic Work with Stress Level f_2

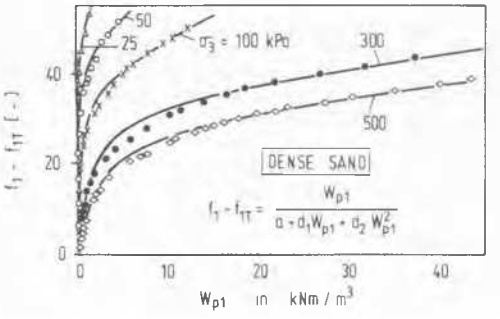

Fig. 4 Variation of Dilative-Plastic Work with Stress Level f_1

$$f_1 - f_{1T} = \frac{W_{p1}}{a + d_1 W_{p1} + d_2 W_{p1}^2}$$

where d_1 is constant and the parameters a and d_2 vary with confining stress (σ_3). These variations can be approximated by exponential functions with constants determined by triaxial compression tests.

The adequacy of a stress-strain model can only be verified by comparison of predicted soil behaviour with laboratory experiments. The capabilities of this stress-strain theory are demonstrated in Fig. 5 and 6. Fig. 5 shows the prediction of the stress-strain and volume change characteristics obtained for dense sand in triaxial compression tests. Fig. 6 indicates the ability to predict stress path dependency. The theory is applicable to general threedimensional stress conditions and models essential aspects of soil behaviour, observed in experimental investigations. The basic soil parameters can be derived entirely from isotropic compression and triaxial compression tests.

The elastoplastic stress-strain matrix $[D^{ep}]$ which is needed to carry out incremental elastoplastic

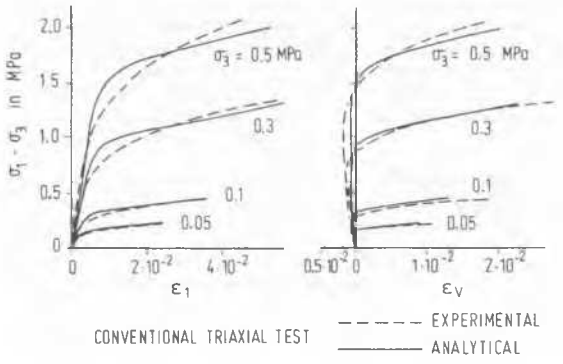

Fig. 5 Comparison of Calculated and Measured Deviator Stress-Strain and Volume Change Behaviour for Triaxial Compression Tests on Sand

finite element analyses, is derived from so called consistency relations. They result from the fact that at any instant both yield surfaces pass through the actual stress point in principal stress space. Thus if

$$F(\sigma_{ij},\ \varepsilon^p_{ij}) = 0$$

we also have

$$F(\sigma_{ij} + \Delta\sigma_{ij},\ \varepsilon^p_{ij} + \Delta\varepsilon^p_{ij}) = 0 \qquad \text{and}$$

$$\{\frac{\partial F_1}{\partial \sigma_{ij}}\}^T\{\Delta\sigma_{ij}\} + \{\frac{\partial F_1}{\partial \varepsilon^{p1}_{ij}}\}^T\{\Delta\varepsilon^{p1}_{ij}\} = 0$$

$$\{\frac{\partial F_2}{\partial \sigma_{ij}}\}^T\{\Delta\sigma_{ij}\} + \{\frac{\partial F_2}{\partial \varepsilon^{p2}_{ij}}\}^T\{\Delta\varepsilon^{p2}_{ij}\} = 0$$

Using the flow rules and the consistency relations, the incremental elastoplastic stress-strain relationship for double hardening materials may be derived. The final form of the relationship may be written as

$$\{\Delta\sigma_{ij}\} = [D^{ep}]\ \{\Delta\varepsilon_{ij}\} \qquad i;j = x,y,z$$

in which $[D^{ep}]$ is the elastoplastic material matrix which may be expressed as

$$[D^{ep}] = [D^e] - [D^e] \cdot \frac{\eta^1 \cdot \Gamma - \gamma^1 \cdot \Omega}{\Gamma \cdot \Lambda - \xi \cdot \Omega}\{\frac{\partial g_1}{\partial \sigma_{ij}}\} -$$

$$- [D^e]\ \frac{\gamma^1 \cdot \Lambda - \xi \cdot \eta^1}{\Gamma \cdot \Lambda - \xi \cdot \Omega}\{\frac{\partial f_2}{\partial \sigma_{ij}}\}$$

where

$$\gamma^1 = \{\frac{\partial f_2}{\partial \sigma_{ij}}\}^T [D^e]$$

$$\eta^1 = \{\frac{\partial f_1}{\partial \sigma_{ij}}\}^T [D^e]$$

are vectors and

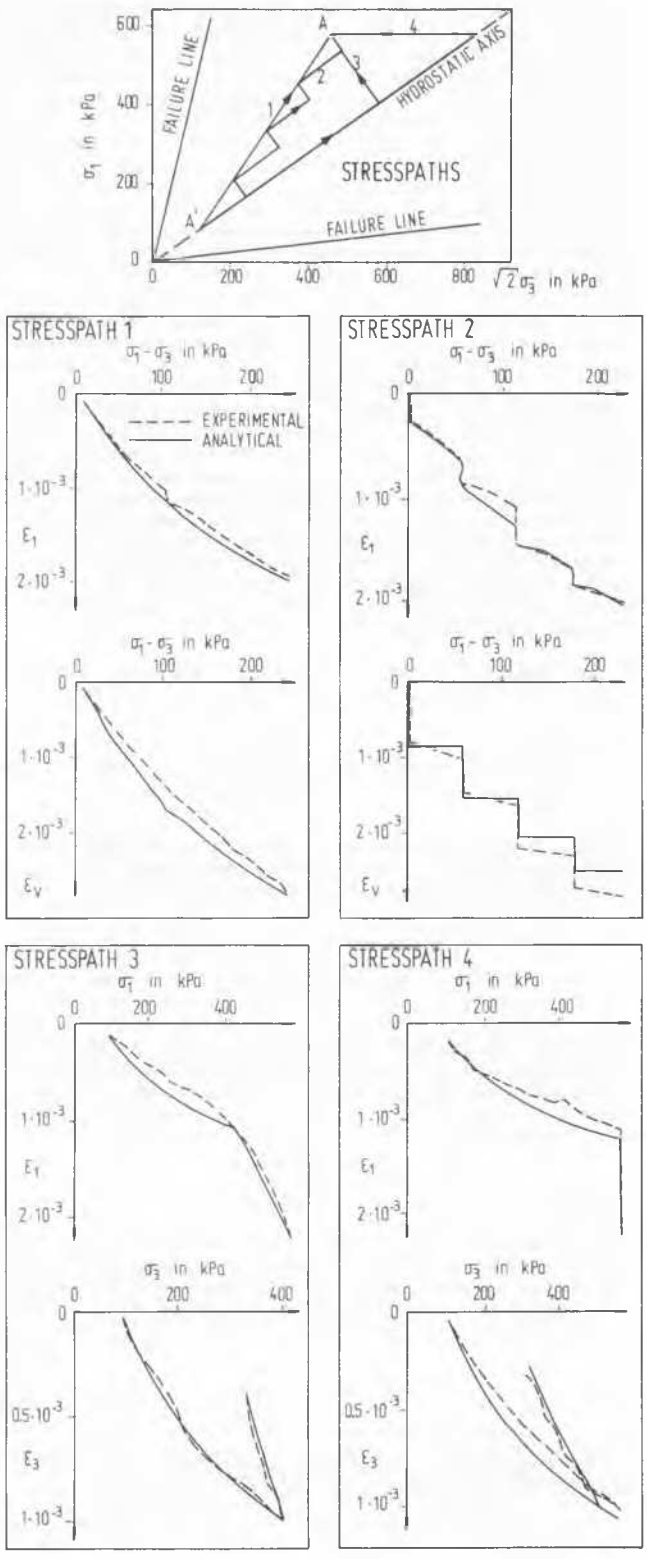

Fig. 6 Comparison of Calculated and Measured Behaviour of Sand for Different Stress-paths in Triaxial Plane

$$\Omega = \{\frac{\partial f_1}{\partial \sigma_{ij}}\}^T [D^e] \{\frac{\partial f_2}{\partial \sigma_{ij}}\}$$

$$\Lambda = \{\frac{\partial f_1}{\partial \sigma_{ij}}\}^T [D^e] \{\frac{\partial g_1}{\partial \sigma_{ij}}\} - \{\frac{\partial f_1}{\partial \varepsilon^{p1}_{ij}}\}^T \{\frac{\partial g_1}{\partial \sigma_{ij}}\}$$

$$\xi = \{\frac{\partial f_2}{\partial \sigma_{ij}}\}^T [D^e] \{\frac{\partial g_1}{\partial \sigma_{ij}}\}$$

$$\Gamma = \{\frac{\partial f_2}{\partial \sigma_{ij}}\}^T [D^e] \{\frac{\partial f_2}{\partial \sigma_{ij}}\} - \{\frac{\partial f_2}{\partial \varepsilon^{p2}_{ij}}\}^T \{\frac{\partial f_2}{\partial \sigma_{ij}}\}$$

are scalars.

$[D^e]$ means the matrix of elasticity. Details of the derivation can be found in Arslan (1980).

SOME ASPECTS OF ANCHORED WALL ANALYSIS

The problem of earth pressure only does not necessitate finite element analyses. Conventional earth pressure theories combined with some experience have proven to be successful and to fulfill requirements of engineering practice in most cases. However, the sole criterion for the suitability of an anchored wall design is vertical and horizontal deformation at ground level. If the influence at ground level has to be considered, the requirements at analytical and numerical aids - finite element analysis included - are much higher.

The ground level behind anchored walls moves downward as long as high prestress of anchors does not produce heave between anchor head and bond length. Finite element analyses with noncohesive soils, published up to now, indicate upward movements behind the wall. Very often only lateral displacements of the wall are discussed and vertical displacements are neglected. The analyses of Huder (1975) with a bilinear-elastic approach yield heave of the same size as lateral wall deformations. Gartung et al. (1978) present heave as a finite element result as well. Egger (1972) applies a simple material model and only discusses earth pressures and wall behaviour. Breth and Stroh (1976) discuss analyses of anchored walls in stiff clay which display settlements in the area behind the bond length of the anchor but heave in the immediate neighbourhood of the wall. Izumi et al. (1976) describe finite element analysis of strutted excavations where heave has been calculated and settlements have been observed. Only finite element analyses with soft cohesive soils with no volume change yield settlements of the ground level behind the wall.

Anchor forces, size of earth pressure and wall deformations can be analysed, but deformations of the ground level have been predicted neither qualitatively nor quantitatively in the past.

EARTH PRESSURE DISTRIBUTION AND ANCHOR FORCES

Geometrical anchor configuration and prestress have a decisive influence on earth pressure distribution. Findings from model tests and in situ observations have been used in the past to draw conclusions concerning the design load figure which has to be applied in the static analysis of walls. In this chapter the authors want to emphasize some aspects of earth pressure distribution. The results presented herein have been obtained numerically by finite element analyses with the constitutive model and the soil parameters discussed in a previous chapter. The discussion is divided into two parts: First, earth pressure distribution and anchor loads at various prestress conditions are presented. The corresponding deformation behaviour will be discussed separately. Usually, for conventional analysis of anchored walls, a three-step procedure has to be performed:

(a) An earth pressure distribution (design load figure) has to be selected.

(b) Anchor loads (reactions) have to be calculated.

(c) The degree of prestress must be chosen.

Step (a) introduces an uncertainty into analysis and design. Depending on soil behaviour, wall stiffness, anchors and excavation procedure, various idealized earth pressure distributions are possible. In practice, the choice is narrowed by personal judgement or by codes. Nevertheless there remains some freedom of choice. Step (b) can be performed in the usual manner of statically indeterminate elastic analysis or plastic analysis. For prestress (step c) normally a degree of 80 % is chosen which means that anchors are prestressed at a level of 80 % of their statically determined load. After these steps have been performed, there is almost no feedback to the engineer as to how the soil-wall-anchor system reacts upon applied prestress in the course of excavation. Here finite element analysis is a valuable tool which allows one to investigate which earth pressure distribution will develop in dependence of applied anchor force. In addition, information about deformations can be obtained.

For the analyses presented here two design load figures have been assumed (Fig. 7): a uniformly distributed load with uniform anchor loads and a triangle load with anchor loads increasing with depth. For uniform load three degrees of prestress have been investigated: 0 %, 80 % and 120 % of analytically determined anchor load. 0 % prestress means that anchors are installed and initially have no tendon force. 80 % prestress is the normal case in construction practice. Over-prestress at 120 % of calculated load is sometimes recommended to reduce deformations, e.g. in the case of sensitive neighbouring structures.

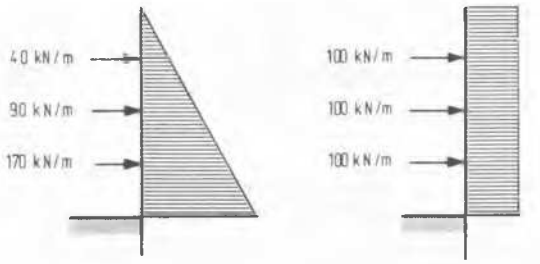

Fig. 7 Design Load Figures

To start a finite element analysis the above mentioned steps (a), (b) and (c) have to be executed. They yield forces and bending moments which permit to design the wall. Fig. 8 shows the geometry of the investigated triple anchored excavation. It is taken as symmetric and in plane strain condition.The moment of inertia of the

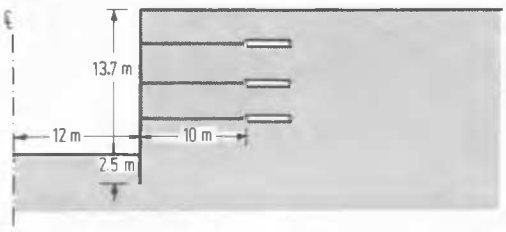

Fig. 8 Geometry of Excavation

wall is 7200 cm^4/m. The anchors have a diameter of 26.5 mm with a permissible anchor load of 340 kN. Soil is represented by 4-node serendipity elements with 3 degrees of freedom. The sheetpile wall consists of beam elements with 3 d.o.f. per node. Anchors are simulated by bar elements. To simulate frictional behaviour between wall and soil, with exactly defined shearstress-shear displacement relations, joint elements are introduced.The excavation is executed step by step in layers of 1.7 m. Each excavation step is divided into various subincrements. At excavation depths of 3.4 m, 6.8 m and 10.3 m anchors are installed and prestressed. These simulation activities are performed automatically in the finite element code (Czapla et al, 1978; Wanninger 1980).

The assumption of uniformly distributed earth pressure for conventional analysis is widely accepted and, for example, allowed according to German recommendations. 80 % prestress is a standard measure as well. Thus, the case of uniform design load and 80 % prestress serves as a reference frame. Fig. 9(a) indicates that prestress according to uniform design load yields an earth pressure distribution which is almost a reflection of prestress. Earth pressure at anchor A, even at the final excavation stage, exceeds K_o-condition. At the height of each anchor a clear maximum can be observed. The dashed lines present intermediate stages of earth pressure after prestress of each anchor. The maximum disappears with the next excavation step. Anchor forces remain almost constant after prestressing. Only the force in deepest anchor C increases significantly. The sum of anchor forces is 347 kN/m. Fig. 9(b) shows that installing anchors without prestress, yields a triangular distribution. Anchor forces increase significantly during excavation. The sum at the final stage is 295 kN/m. Prestressing at 120 % - Fig. 9(c) - yields an

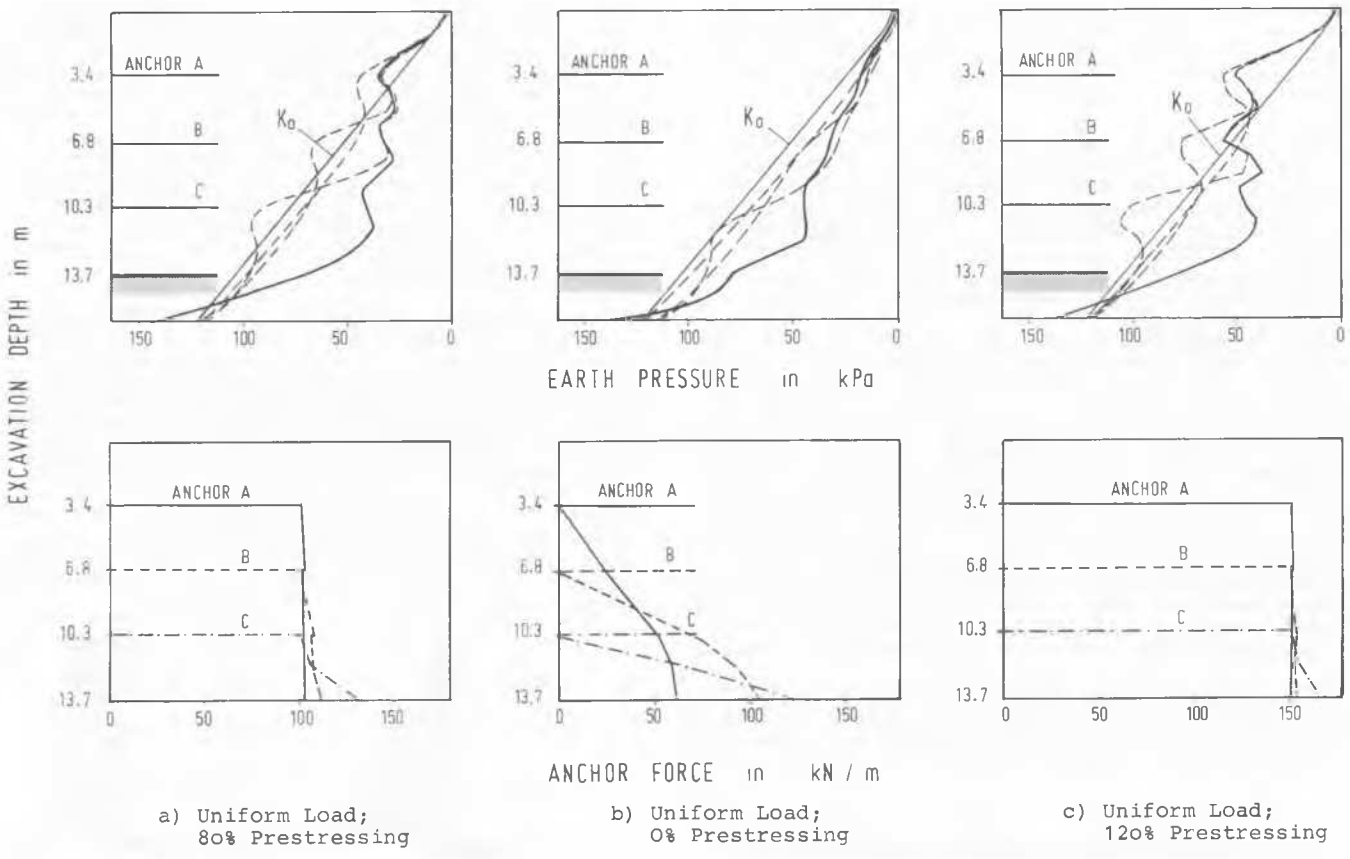

Fig. 9 Earth Pressure and Anchor Forces for Different Degrees of Prestressing at Various Excavation Stages

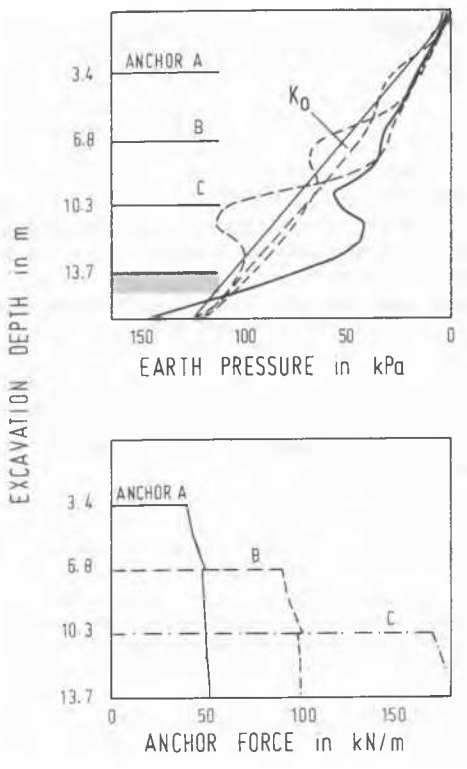

Fig. 10 Earth Pressure and Anchor Forces for Triangle Prestress at Various Excavation Stages

earth pressure distribution qualitatively similar to Fig. 9(a) but with higher absolute values. The anchor forces, which have a sum of 470 kN/m, again do not vary much after prestressing. The assumption of a triangle load leads to anchor loads increasing with depth (Fig. 10). The numerically obtained earth pressure is again a mirror image of prestress.As a conclusion it may be said that earth pressure distribution and anchor loads reflect exactly the design load figure and the degree of prestressing. This means that any distribution may be achieved by constructional measures. However, a discussion of deformations is necessary.

DEFORMATION BEHAVIOUR

The wall with uniformly distributed load and 80 % prestress moves laterally up to 2 cm with a maximum at the deepest anchor (Fig. 11a). Prestress according to a triangle design load yields the same amount of wall displacement with the maximum at the top of the wall (Fig. 11b). Prestress of 120 % reduces lateral movements to 1.5 cm (Fig. 11c). Deformation characteristics remain unchanged. Installing anchors without prestress (Fig. 11d) leads to considerable horizontal movements up to 6.5 cm.

Deformations at ground level are the most interesting factor for judgement of soil-structure interaction. 80 % prestressing with uniform load (Fig. 12a) leads to almost uniform settlements of 0.6 cm between wall and the end of the anchors. The dashed lines represent deformations during excavation. 80 % prestress with a triangle load figure does not yield a significantly different settlement behaviour (Fig. 12b). Prestress at 120 % (Fig. 12c) reduces settlements to zero at the wall and to 0.7 cm as a maximum. It can be observed that the high degree of prestress evokes upward movements of the ground level at intermediate construction phases. 0 % prestressing (Fig. 12d) yields settlements of 5 cm with a 1:400 slope of settlement trough. Together with horizontal displacements of 6.5 cm (Fig. 11d) it indicates that prestress of anchors is mandatory to avoid damage in neighbouring structures.

CONCLUSIONS

Initial assumptions and construction measures in the design of multiple-anchored walls offer a variety of possibilities to adapt this method to practical requirements. It is shown that earth pressure distribution is totally dominated by prestress and by the choice of design load figures. Almost any desired distribution may be

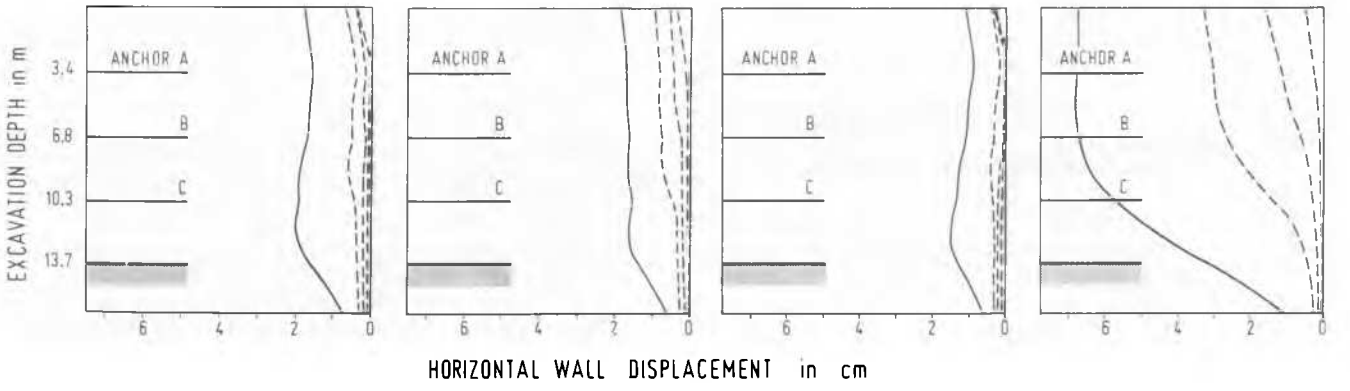

a) Uniform Load; 80% Prestressing
b) Triangle Load; 80% Prestressing
c) Uniform Load; 120% Prestressing
d) Uniform Load; 0% Prestressing

Fig. 11 Horizontal Wall Displacement for Different Load Figures and Degrees of Prestressing

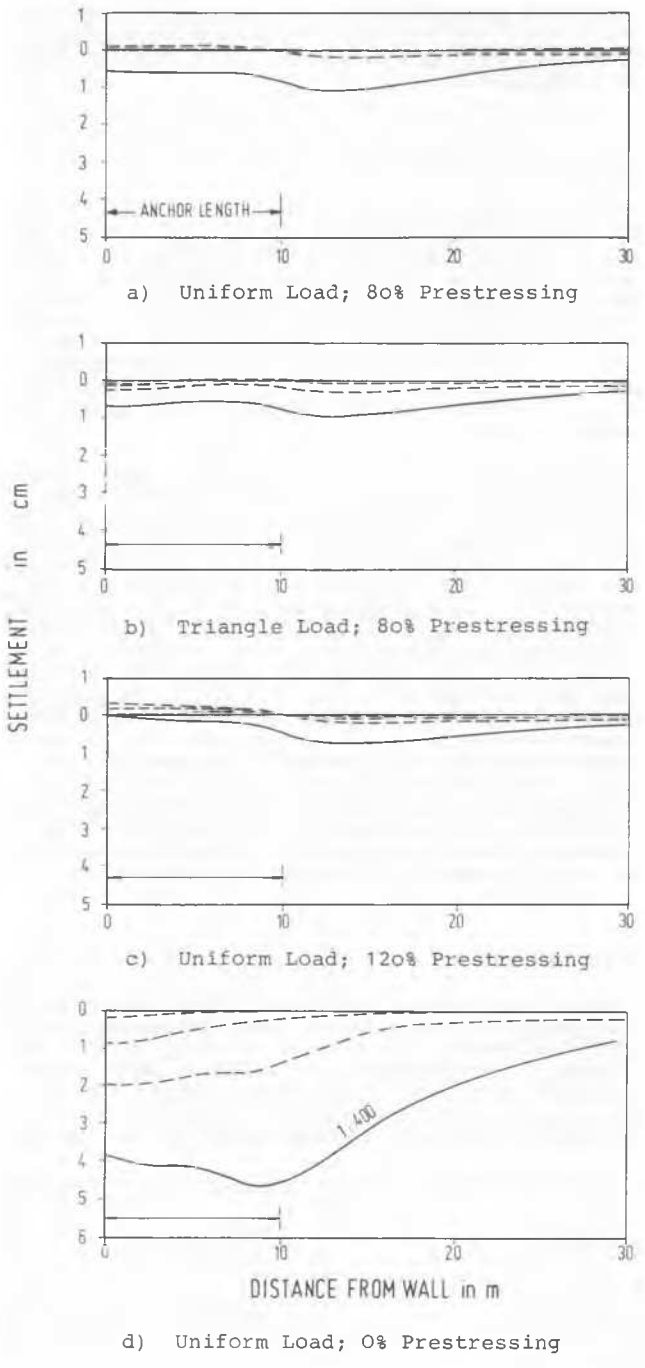

Fig. 11 Settlements for Different Load Figures and Degrees of Prestress

achieved. Deformation behaviour can be influenced as well. It is obvious that the amount of prestress force is more important to reduce settlements than the form of the design load figure. Thus, numerical analysis proves to be a useful tool for engineering judgement of construction procedures. However, the application of correct constitutive laws is important.

REFERENCES

Arslan, U. (1980): Zur Frage des elastoplastischen Verformungsverhaltens von Sand. Mitt. VA Bod.mech. u. Grundbau TH Darmstadt 23.

Breth, H., Stroh, D. (1976): Ursachen der Verformung im Boden beim Aushub tiefer Baugruben und konstruktive Möglichkeiten zur Verminderung der Verformung von verankerten Baugruben. Der Bauingenieur 51, 81-88.

Breth, H., Wolff, R. (1976): Versuche mit einer mehrfach verankerten Modellwand. Die Bautechnik 53, 38-42.

Breth, H., Chambosse, G., Arslan, U. (1978): Einfluß des Spannungsweges auf das Verformungsverhalten des Sandes. Geotechnik 1, 2-9.

Czapla, H., Katzenbach, R., Rückel, H.,Wanninger, R. (1978): Manual zum FE-Programmsystem STATAN-15 und Graphischen DV-System PLOSYS. Fachgebiet Bod.mech. u. Grundbau TH Darmstadt.

Egger, P. (1972): Influence of Wall Stiffness and Anchor Prestressing on Earth Pressure Distribution. Proc. 5th Europ. Conf. Soil Mech. Found. Eng. Madrid, 259-264.

Gartung, E., Bauernfeind, P., Bianchini, J. C. (1978): Spannungs-Verformungsberechnung für eine Rückverankerte Baugrubenwand im Keupersandstein. Veröff. Grundbauinst. LGA Bayern 34.

Gudehus, G. (1973): Elastoplastische Stoffgleichungen für trockenen Sand. Ingenieur-Archiv 42, 151-169.

Hill, R. (1950): The Mathematical Theory of Plasticity. Clarendon Press, Oxford.

Huder, J. (1975): Tiefe Baugruben. Erddrücke und Deformationen. Mitt. Schweiz. Ges. Bod.Felsmech. 92, 1-10.

Izumi, H., Kamemura, K., Sato, S. (1976): Finite Element Analysis of Stresses and Movements in Excavations. Proc. 2nd Int. Conf. Num. Meth.Geomech. Blacksburg, 701-712.

Lade, P. V., Duncan, J. M. (1973): Cubical Triaxial Tests on Cohesionless Soils. ASCE J. Soil Mech. Found. Div. Vol. 99 SM10, 793-811.

Lade, P. V., Duncan, J. M. (1975): Elastoplastic Stress-Strain Theory for Cohesionless Soil. ASCE J. Geot. Div. Vol. 101 GT10, 1037-1053.

Lomize, G. M., Kryzhanovsky, A. L. (1967): On the Strength of Sand. Proc. Geot. Conf. Oslo Vol. I, 215-219.

Matsuoka, H., Nakai, T. (1977): Stress-Strain Relationship of Soil Based on the SMP. Proc. Specialty Session 9, 9th Int. Conf. Soil Mech. Found. Eng. Tokyo, 153-162.

Roscoe, K. H. (1970): The Influence of Strains in Soil Mechanics. 10th Rankine-Lecture, Geotechnique 20, 129-170.

Wanninger, R. (1980): Zur Lösung von Grundbauaufgaben mit Hilfe von elastoplastischen Stoffgesetzen vorgeführt am Einzelfundament und an der verankerten Wand. Mitt. der VA Bod.mech. u. Grundbau TH Darmstadt 23.

Wanoschek, R., Breth, H. (1972): Auswirkung von Hauslasten auf die Belastung ausgesteifter Baugrubenwände. Straße Brücke Tunnel 24, 197-200.